Renewable Energy 179 (2021) 248–261

Contents lists available at ScienceDirect

Renewable Energy

journal homepage: www.elsevier.com/locate/renene

A two-stage processing of cherry pomace *via* hydrothermal treatment followed by biochar gasification

Mariusz Wądrzyk [a, b, *], Przemysław Grzywacz [a], Rafał Janus [a, b], Marek Michalik [c]

[a] AGH University of Science and Technology, Faculty of Energy and Fuels, A. Mickiewicza Av. 30, 30-059, Kraków, Poland
[b] AGH University of Science and Technology, AGH Centre of Energy, Czarnowiejska 36, 30-054, Kraków, Poland
[c] Jagiellonian University, Institute of Geological Sciences, Gronostajowa 3a, 30-387, Kraków, Poland

ARTICLE INFO

Article history:
Received 1 March 2021
Received in revised form
21 May 2021
Accepted 28 June 2021
Available online 1 July 2021

Keywords:
Cherry pomace
Industrial waste valorization
Hydrothermal treatment
Biochar
Gasification
Sustainability

ABSTRACT

Poland is the EU's largest producer of cherry, which largely is further processed. As a consequence, a problematic waste – cherry pomace – is generated as by-product. Among the new sustainable technologies for organic waste valorization particularly perspective are thermochemical methods, which can be divided into conventional one, i.e., dry route (e.g. pyrolysis, gasification) and wet route (i.e. hydrothermal treatment). Herein, we proposed a two-stage thermochemical processing route for the conversion of cherry pomace, i.e., hydrothermal treatment followed by CO_2 gasification. Firstly, we transformed the feedstock into biochar *via* hydrothermal processing. The aim of this stage was to analyze the effect of processing temperature (200–350 °C) on the distribution of the yield of various groups of products. The residual biochar was obtained with the highest yield (33–57 wt%). Among the gas-phase products, the dominant constituent was CO_2. The upgrading of the biochars through gasification with CO_2 to ensure the sustainability of conversion was the subsequent step. The quality of the biochars was examined by infrared spectroscopy, proximate and ultimate analysis, SEM, and low-temperature nitrogen adsorption. The activation energy ranged between 668 and 732 kJ mol^{-1} for the gasification of the biochar prepared at 275 and 200 °C, respectively. It was found that biochars produced at different conditions exhibit various properties as a result of gradual degradation of the original components of the raw material and increase in aromaticity occurring with the increase in the processing temperature.

1. Introduction

Global development results in the appearing of new trends in society. One among them is the popularity of a healthy lifestyle, which drives the increasing consumption of different kinds of fruits, vegetables and juices. It has to be mentioned that Poland is the main producer of many kinds of fruits, e.g. cherries among the European Union [1]. Estimated fresh cherries production in the EU was above 738 thousand tonnes in the 2019/2020 marketing year, while Poland alone reached 195 thousand tonnes [2]. Moreover, Poland is also the EU's largest cherry manufacturer, transforming ca. 75% of its production [2]. It is worth noting that this tendency finds reflection in the statistics depicting the production of various kinds of juices and nectars in Poland between 2007 and 2015, when it systematically increased and annually ranged from 1386.5 mln litres to 1585.0 mln litres [3]. The natural consequence of this trend is the increasing amount of waste biomass generated by the food industry. These wastes exhibit high content of water (the so-called wet residues). Examples of such residuals are fruit and vegetable pomaces generated as a by-product in juice and jam factories. As a result of considerable quantities of this kind of raw material on the market, new, more effective and sustainable concepts of its utilization are being developed. For instance, in the literature can be found reports concerning the usage of fruit and vegetable pomaces towards obtaining bioactive compounds [4], value-added compounds like organic acids [5,6], natural antioxidants as food additives [7–10], dietary fibres [11,12], biopolymers [13,14], and recently also for biofuels production and bioenergy generation [15–17].

On the other hand, according to the new Renewable Energy Directive (RED II) in forthcoming years, the share of advanced biocomponents produced from non-edible raw materials, e.g. waste biomass and industrial residues, should be progressively

* Corresponding author. AGH University of Science and Technology, Faculty of Energy and Fuels, A. Mickiewicza Av. 30, 30-059, Kraków, Poland.
E-mail address: wadrzyk@agh.edu.pl (M. Wądrzyk).

https://doi.org/10.1016/j.renene.2021.06.130

increasing (3.5% in the transport sector until 2030) [18]. One of the most perspective group of methods for wastes transformation into value-added drop-in fuels' component is the thermochemical route. It is characterized by a high conversion rate and relatively short processing times [19]. Among them, the conversion of various types of biomass *via* pyrolysis and gasification has been widely investigated recently [20–28]. However, it has to be mentioned that prior to both processes the feedstock should be dried to reduce the moisture content to no more than a dozen percentage, what in the case of mentioned residues from the food industry is troublesome. Thus, it is reasonable to apply proper pretreatment before the main conversion. In the case of wet residues (like pomace, algae, sewage sludge) which often contain abundant amounts of water, direct conversion *via* pyrolysis or gasification could not be economically justified because of the high value of latent heat of evaporation for water. For such a kind of raw materials, particularly promising is the conversion occurring in near-critical conditions of water called hydrothermal treatment (HTT), which allows omitting the drying step. HTT is a process of chemical transformation of biomass, carried out in the presence of water at elevated temperature and under high pressure. Water, as an environmental friendly reaction medium which exhibits unique properties, poses an excellent environment for biomass conversion. In the subcritical region of water (critical point: $T_{cr.} = 374$ °C; $p_{cr.} = 22.115$ MPa), its dissociation constant rises drastically, causing water to act as an acid or base catalyst for numerous reactions and empowering the chemical conversion of almost all types of organic compounds *via* hydrolysis and ionic reactions [29–31]. As a result of those conversions, four groups of products are obtained: (I) solid fuel called biochar, (II) gas products, (III) nonpolar liquid organics called biocrude, and (IV) polar organics dissolved in water. The process occurring between ca. 180–250 °C called hydrothermal carbonization, aims to the maximization of biochar production, while the conditions closer to the critical point of water are beneficial when the process target product is liquid biocrude. However, even in the case of hydrothermal liquefaction range, the biochar yield remains abundant, reaching usually up to several dozen percent. Recently, hydrothermal processing was used by plenty of researchers for the conversion of various raw materials towards the production of different groups of bioproducts and it can be concluded that in the case of wet-type biomass it seems to be a more reasonable technology than direct pyrolysis or gasification [30,32–35]. Interestingly, the biochar obtained after hydrothermal pretreatment exhibits a more hydrophobic surface that, in turn, facilitates mechanical dewatering (if necessary) [36,37] and could be beneficial for its further upgrading. Consequently, such biochar stands as an excellent candidate for further conversion *via* conventional thermochemical methods (pyrolysis, gasification).

Nowadays, wet residual matter from the food industry does not find a perspective application route, and the most common utilization method is its usage as a feed or fertilizer. According to Dhillon et al. [4], only 20% of pomace is used as animal feed, while the rest is utilized in a non eco-friendly way like landfilling, incineration, or composting. Naturally, the consequence is an increasing greenhouse gases emission to the atmosphere. More importantly, the big scale of production and processing of fruit and vegetables in Poland as well as its low biochemical stability, and the possibility of rapid different microorganisms growth (also hazardous) enforces seeking for a new sustainable approach for the conversion of those troublesome waste residuals. Thus, herein we proposed a two-stage processing route for the conversion of cherry pomace as an exemplary high-moisture-containing material (Fig. 1). In this approach, the first stage is based on hydrothermal treatment of raw material to obtain high quality and high yield of biochar as the desired product. Subsequently, in the second stage, the resultant biochar is subjected to gasification. The latter one is a thermochemical conversion in which occurs the partial oxidation of solid biomass into a gaseous high-energetic product at a temperature range between 800 and 1000 °C. The main product of gasification is the gas mixture called synthetic gas (or syngas), which is rich in CO and H_2. It is worth emphasizing that the resultant syngas offers better flexibility in finding the most beneficial application route (liquid fuels manufacturing by Fischer-Tropsch process, chemicals, power generation) compared to pyrolysis products. The gaseous fraction of hydrothermal treatment is composed in the majority of CO_2, so to ensure the sustainability of the whole technology, we consider subsequently the gasification of the resultant biochar under the atmosphere of carbon dioxide as a gasification medium. The biocrude in the presented approach is devised as an internal source of heat within the technology. However, it is worth emphasizing that the mentioned liquid mixture could be also considered as a source of value-added chemicals, thus its application potential should be also evaluated, as what was herein also done. The scientific literature research discloses a few multistage approaches towards different kinds of biomass transformation, e.g., Refs. [38,39]. However, to the best of our knowledge, there is a lack of any research on the utilization of fruit pomace consentient with the approach proposed here. Indeed, the present contribution is the first report regarding the processing of cherry pomace in subcritical water. Additionally, it is also important to highlight that we have also studied the possibility of direct conversion of as-received industrial wet wastes employing subcritical water. Such an approach could pave the way for the development of new sustainable technology for the valorization of wet residues and simplify the entire processing procedure.

The present paper brings new insights into the valorization of cherry pomace as industrial waste. The untapped cherry pomace was chosen as a promising feedstock for inexpensive and environmentally friendly manufacturing of bioproducts *via* the proposed two-stage thermochemical concept. The main aim of the present research was to investigate the effect of hydrothermal treatment temperature (tested within the range 200–350 °C) on the yield and quality of the resultant biochar and its possibility for further conversion into synthetic gas *via* gasification with CO_2. The studied biochar was obtained by carrying out a series of tests in subcritical conditions of water. The quality of biochar was analyzed by means of elemental analysis (EA), thermogravimetric analysis (TG), scanning electron microscopy (SEM), nitrogen adsorption and diffuse reflectance infrared Fourier transform spectroscopy (DRIFT). The final stage was the investigation of the gasification kinetics of HTT biochars obtained at various conditions. Additionally, the composition of other groups of products obtained through hydrothermal treatment was also investigated. Furthermore, we also focused on the investigation of the changes in the mineral matter composition upon the liquefaction process with regard to raw material, which could result in attenuation of the catalytic effect during gasification.

2. Materials and methods

2.1. Raw material

The cherry pomace used in this research is leftover from the industrial juice production facility – it has been supplied by Tymbark - MWS company, Poland. The as-received feedstock was a mixture of residual seeds, leafs, stalks, and cherry peel, therefore before subjecting to thermochemical conversion it was homogenized. For this purpose, the raw material was ground using Fritsch Pulverisette 15 mill to the mesh fraction of ca. <2 mm. The prepared raw material was kept sealed in plastic bags stored frozen at −18 °C.

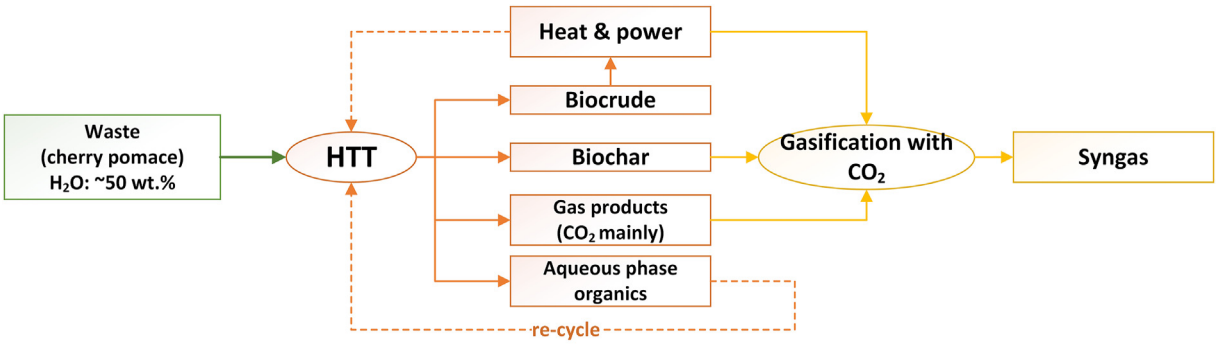

Fig. 1. An approach for sustainable two-stage processing of waste cherry pomace towards syngas.

The authors have not noticed any indication of biological degradation of feedstock subjected to tests. The moisture and ash content in the raw material were equal to 52.21 wt% and 0.99 wt%, respectively. The elemental composition of raw cherry pomace was presented in Table 2.

2.2. Hydrothermal treatment procedure

The hydrothermal treatment tests were conducted in a 500 cm^3 Parr 4575A (USA) batch reactor equipped with a Parr 4848 temperature controller (USA). Prior to each experiment, a gas tightness test was carried out by pressurizing the reactor with nitrogen (grade 5.0, p = 10 bar). Typically, approximately 100 g of cherry pomace prepared before as water slurry was placed in the reactor under a nitrogen atmosphere ($p_0 = 5$ bar). The concentration of the dry biomass in the slurry was kept constant at 10 wt%. The proper concentration was adjusted by dilution of the as-received slurry with distilled water. The processing temperature was set in the range of 200–350 °C. The reaction was carried out under an autogenous pressure, so it corresponded to the real operational pressure between ca. 40–150 bar. Depending on the set process temperature, the time to reach the desired temperature varied between 30 and 40 min. The reaction time, defined as a holding time between reaching the set temperature and starting cooling down, was 30 min. The autoclave was equipped with an internal water cooling coil (single loop) which provided controlling temperature (minimization of its fluctuations) during tests as well as cooling the reactor at the end thereof. Additionally, for cooling after the test, we used also and external small air fan to increase the cooling rate. The total cooling time to ambient temperature varied between ca. 45–60 min (depending on the processing temperature). After the reactor was cooled down, the gas pressure was recorded, and a sample was taken for analysis. Then, the autoclave was depressurized and the products were transferred into the collector.

To separate and recover the bioproducts from as-received reaction mixture, the standard procedure of extraction with dichloromethane (DCM; Sigma Aldrich, 99.9%) followed by vacuum filtration and drying was employed, according to the method reported elsewhere [40]. The applied recovery procedure allowed for obtaining dry and impurities-free biochar. As a result, four groups of products were obtained: (I) biocrude as a mixture of DCM-soluble organics; (II) water phase containing dissolved polar organics; (III) gas products; and (IV) biochar. The yield of gas products was calculated according to the ideal gas law, based on the temperature and pressure measured inside the reactor. Each phase of HTT product was recovered quantitatively and analyzed separately to estimate the yield as well as analyze the properties and chemical composition of each fraction experimentally.

2.3. Analytical procedures for HTT bioproducts characteristics

2.3.1. Elemental analysis (EA)

Elemental analysis (C, H, N) of the studied feedstock and produced biochars was carried out using a Thermo Scientific Flash 2000 apparatus. The oxygen content was determined by subtracting the summary percentages of ash, C, H, and N elements from 100%. Each run was repeated thrice, and the present result is the average value.

2.3.2. Diffuse reflectance infrared Fourier transform spectroscopy (DRIFT)

The qualitative composition of the obtained biochars and biocrudes was investigated by means of mid-infrared Fourier-transform spectroscopy. The spectra were collected on a Nicolet iS5 (Thermo Scientific) spectrometer equipped with a DRIFT device (EasiDiffTM-Pike Technologies) and an attenuated total reflectance device (ATR) with a diamond crystal and DTGS detector. For each spectrum, sixteen scans were recorded at a wavenumber region of 400–4000 cm^{-1} at a resolution of 4 cm^{-1}. The biochars were analyzed using DRIFT technique and prepared as 1 wt% mixtures with KBr, while biocrudes were analyzed using ATR technique without pretreatment.

2.3.3. Scanning electron microscopy (SEM)

SEM images were taken on a HITACHI S-4700 field emission microscope at an accelerating voltage of 20 kV. Samples were prepared by mounting the powder onto a conducting adhesive carbon disc. To reduce the charging effect, the materials were coated with an Au layer.

Table 1
The procedure of the TG kinetic measurements.

Step 1 - Stabilization	Step 2 – Measurement	Step 3 - Ending
Initial conditions were stabilized, i.e., pressure at 10 bar, carbon dioxide flow at 200 cm^3 min^{-1}	Temperature was ramped from ambient up to 1000 °C at a heating rate 3 °C min^{-1} and a constant flow of CO_2 set at 200 cm^3 min^{-1}	Heating was turned off, the CO_2 flow was kept at 100 cm^3 min^{-1} to purge and cool down the reactor zone

2.3.4. Low-temperature nitrogen adsorption

Nitrogen adsorption–desorption isotherms were recorded at −195.8 °C using a Micromeritics ASAP 2020 apparatus. Prior to the measurements, the samples were evacuated at 100 °C for 5 h under vacuum. Specific surface areas were calculated based on the BET model. Total pore volumes (V_t) were assessed from the amounts of nitrogen adsorbed at a relative pressure of 0.99, while micropore volumes (V_{mi}) were estimated using the *t*-plot model. Pore size distributions were calculated using the 2D-NLDFT model devised for carbons with heterogeneous surfaces (SAIEUS 3.0 software).

2.3.5. Gas chromatography coupled to mass spectrometry (GC-MS)

The qualitative analysis of a volatile fraction of HTT biocrude was carried out using a GC-MS Agilent apparatus GC 7890B equipped with a MS 5977A mass spectrometer and DB-17 capillary column (30 m × 0.32 mm × 0.5 μm). The samples were prepared as 5 wt% solution in dichloromethane (Avantor Performance Materials, Poland; HPLC grade) and additionally filtered through 0.2 μm PTFE syringe filters (Watson) prior to injection. The obtained MS spectra were interpreted based on the reference MS library (chemical base G1034C). The contributions of the detected compounds were computed relatively as a ratio of the peak area of particular compounds to the summary peak area of all detected components. The detailed information about applied conditions were reported previously [22].

2.3.6. Gas chromatography (GC)

The composition of the HTT gas phase was analyzed using a gas chromatograph (GC-SRI, model 302, SRI-Instruments) equipped with FID and TCD detectors. The separation of constituents was done using HayeSep D packed column with a length of 2 m.

2.3.7. HHV, energy recovery and distribution of C element

The higher heating values (HHV) of the obtained HTT groups of products from cherry pomace were assessed based on the elemental composition according to the empirical Boie's formula. Energy recovery (*ER*) in the form of each HTT group of products (i.e., biochar, biocrude, gas phase, and water-soluble organics) was calculated based on their yields and heating values regarding the energetic value of dry feedstock (Equation (1)).

$$ER_i = \frac{Y_i \cdot HHV_i}{HHV_{feedstock}} \quad (1)$$

ER_i – energy recovery in form of HTT group of products, where *i* means biocrude, biochar, gas phase, or water soluble organics.
Y_i – yield of the *i*-group of products
HHV_i – higher heating value of *i*-group of products

Similarly, the C element distribution in a certain HTT groups of products was calculated as a ratio of the product of yield and C content in each group of products to the content of C element in dried raw material (Equation (2)).

$$C_{share,i} = \frac{Y_i \cdot C_i}{C_{feedstock}} \quad (2)$$

$C_{share,i}$ – yield of C element in the *i*-group of products.

$C_{i/feedstock}$ – C element content in the *i*-group of products or feedstock.

2.4. Biochar gasification procedure and methodology of kinetic analysis

The TG measurements have been carried out using DynTHERM Thermogravimetric Analyzer (Rubotherm, Germany). The fully automated instrument combines two basic systems: (I) the system of the Sartorius Magnetic Suspension Balance coupled to the reactor, where the main measurement occurs, and (II) the reactant-gas dosing system, supplying gases at a given flow and pressure to the reaction zone. During the thermogravimetric measurements, carbon dioxide (grade 4.8) has been used. The measurements were performed under the operational pressure of 10 bar. In each measurement, an amount of 50 mg of biochar's sample of the mesh fraction <0.1 mm was placed in the crucible made of alumina, transferred to the reactor, and subjected to the experimental procedure consisting of three stages as summarized in Table 1.

Based on the data recorded during the TG measurement, the order of the gasification reaction, *n*, was determined. Then, the kinetic parameters, i.e., activation energy (E_a) and pre-exponential factor (A), were calculated using the approximation proposed by Coats and Redfern [41,42]. The reaction order was determined by employing the rate law written as follows:

$$\frac{d\alpha}{dt} = k \cdot (1 - \propto)^n \quad (3)$$

$$\alpha = 1 - \frac{m}{m_0} \quad (4)$$

α the progress of the reaction.
m the current mass of the sample, mg,
m_o initial mass of the sample, mg.

The rate constant k appearing in Equation (3) can be expressed by the Arrhenius equation:

$$k = A \cdot \exp\left(-\frac{E_a}{RT}\right) \quad (5)$$

A pre-exponential factor, 1 min^{-1}.
E_a activation energy, kJ mol^{-1},
R universal gas constant, J $(mol\ K)^{-1}$,
T temperature, K.

In the case of non-isothermal experiments, temperature is changing with time, and the relationship between them is governed by the heating rate $\beta = dT/dt$, which remains constant throughout the experiment. Combining Equations (3) and (5) and introducing β allows to define the n-th order non-isothermal reaction model:

$$\frac{d\alpha}{(1-\alpha)^n} = \frac{A}{\beta} \cdot \exp\left(-\frac{E_a}{RT}\right) dT \quad (6)$$

The left-hand side of Equation (6) may be integrated, while the right-hand side cannot be integrated analytically. The solution is to give an approximation as a series and then truncate it after a small number of the terms. Under such assumptions, the results for $n \neq 1$ can be expressed as follows:

$$\ln\left[\frac{1-(1-\alpha)^{1-n}}{(1-n)T^2}\right] = \ln\frac{AR}{\beta E_a}\left(1 - \frac{2RT}{E_a}\right) - \frac{E_a}{RT} \quad (7)$$

For majority reactions $E_a >> RT$ and the term $\ln\frac{AR}{\beta E_a}\left(1-\frac{2RT}{E_a}\right)$ in Equation (7) can be considered to be constant. Therefore, the Equation (7) was put in the linear form and the value of reaction order n giving the best fit to the experimental data was determined. In the next step, the kinetic parameters, i.e., activation energy E_a and pre-exponential factor A, were calculated.

3. Results & discussion

3.1. Effect of hydrothermal treatment on products yield

The yield distribution of products obtained through the hydrothermal treatment of cherry pomace in the tested range of processing temperature (200–350 °C) is shown in Fig. 2. It can be seen that processing temperature is a meaningful variable affecting the decomposition of the processed pomaces. More specifically, the change of this parameter in subcritical conditions of water causes noticeable changes in the resultant product yield distribution. At lower processing temperatures, the dominant bioproduct is a solid residue called biochar. It could mean that these conditions are beneficial for the production of carbonized hydrochar due to the initiated decomposition of macromolecules like hemicellulose and cellulose. It can be seen that further gradual increase in processing temperature results in a decrease in the yield of solid biochar from ca. 57 to ca. 34 wt%, for 200 and 350 °C, respectively. It is worth noting that above 275 °C, a further decrease in solid residue production is less dynamic, so up to this temperature the majority of macromolecules undergo the conversion. The noted biochars yield are in line with the previous reports regarding hydrothermal treatment of blackcurrant pomace [43], olive pomace [44], as well as grape pomace [45]. The biocrude yield varied in the range of 10–20 wt% for the tested range of conditions. The highest share of biocrude was noticed at moderate temperatures (275–300 °C). Higher temperatures during HTT promote liquid production due to harsher conditions and altered properties of water as solvent. These findings are in line with the values previously reported for lignocellulosic biomass [46–48]. The yield of water-soluble organics was approximately equal to 7–11 wt%. The change of process conditions into more severe regions caused a gradual increase in the gaseous phase share, probably due to the partial secondary decomposition of another group of products, i.e. biocrude and water-soluble organics. The yield of gas products increased from 2 wt% to 18 wt% along with the temperature increase from 200 to 350 °C, respectively.

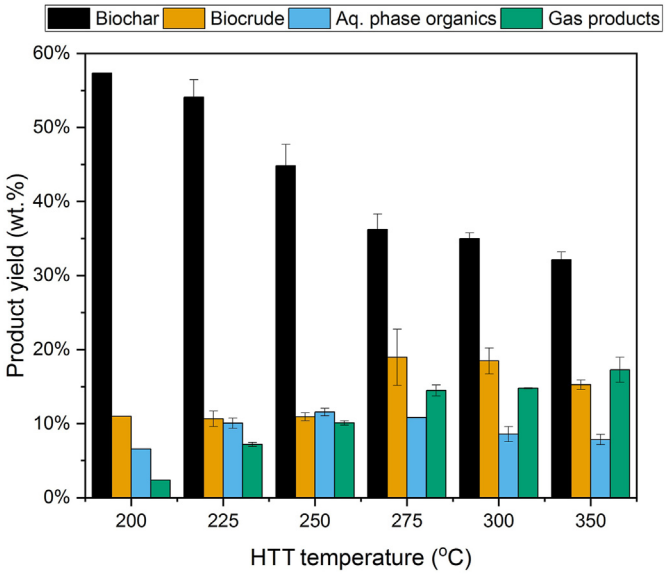

Fig. 2. Hydrothermal treatment products yield distribution as a function of the processing temperature.

3.2. Characteristics of HTT biochar

3.2.1. Elemental analysis

The resultant biochars were dark-colored solid carbonaceous materials. The increase in processing temperature resulted in a gradual darkening of their color, i.e., this one obtained at 200 °C was light brown, while at 350 °C became almost black, which suggested a progressive conversion of the raw structure at glance. The images of the obtained biochar fractions are presented in Fig. 3.

The carbon content in the biochars is higher than for the feedstock and varies from 56.52 to 74.22 wt% for the samples obtained at 200 and 350 °C, respectively. For comparison, the carbon content in dried cherry pomace was 49.22 wt%. Additionally, the oxygen content in HTT biochars is much lower than in the original cherry pomace. In the case of biochar obtained at 350 °C the oxygen decreased by more than 2.5 times. Thus, it can be seen that during conversion in subcritical water, especially at more severe conditions, intensive deoxygenation reactions occur. However, it is worth noting that for biochar produced at 200 °C the oxygen content decreased to a lesser extent compared to the other ones, and it is characterized by only minute lower H content. The further increase in processing temperature led to a reduction of H content to 4.27 wt %. Thus, the dehydration reaction occurs more easily in harsh conditions. In Table 2, the results of the elemental compositions and proximate analysis of raw material and biochars obtained at various temperatures, i.e., 200, 275, and 350 °C, were collected. It can be noticed that hydrothermal treatment of cherry pomace resulted in a decrease in volatile matter of biochars by almost 50%, with a noticeable effect of increasing temperature on its gradual decrease. Simultaneously, the fixed carbon content in biochars increased by 25%, 123%, and 137% for 200, 275, and 350 °C,

Table 2
Elemental composition and proximate analysis of raw materials, HTT biochars and biocrudes obtained from cherry pomace and reference biochar [49] and coal as a fossil fuel [50].

Element/Constituent [wt%]	Raw cherry pomace	HTT – biochar			HTT – biocrude			HTC - biochar from *Virginia mallow* [49]	Coal[a] [50]
		200 °C	275 °C	350 °C	200 °C	275 °C	350 °C		
C[d]	49.22	56.52	68.82	74.22	65.39	70.10	71.40	58.30	61.86
H[d]	6.44	6.16	5.04	4.27	7.90	8.37	9.04	5.67	4.11
N[d]	1.19	0.96	2.31	2.46	2.35	1.98	2.29	0.38	1.03
O[d]	42.16	35.53	21.36	16.24	24.36	19.55	17.27	35.09	10.76
A[d]	0.99	0.83	2.47	2.81	–	–	–	0.58	20.9
VM[d]	74.20	68.07	42.31	38.37	–	–	–	73.89	32.8
FC[d]	24.81	31.09	55.22	58.82	–	–	–	25.53	46.3

[d] - dry basis; [a] -average value from Ref. [50]; A – ash; VM – volatile matter; FC – fixed carbon.

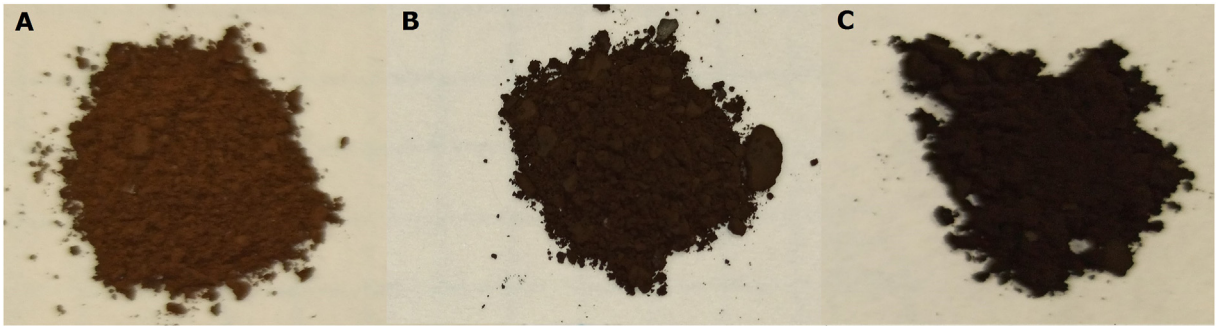

Fig. 3. Photographs of the HTT biochars obtained at different processing temperatures (A) 200 °C (B) 275 °C (C) 300 °C.

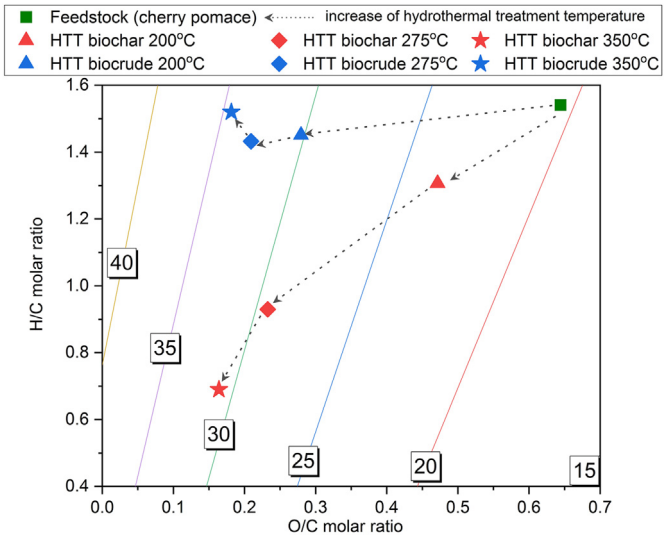

Fig. 4. Comprehensive van Krevelen diagram for the studied HTT biochars and biocrudes obtained at different processing temperatures.

respectively, what is beneficial for further downstream processing of the biochars through gasification. Additionally, comparison of biochars produced from other biomasses – e.g., *Virginia mallow* (dedicated energy crop) [49] in similar conditions showed very close chemical composition. It is also worth noting that biochars obtained at 275 and 350 °C exhibit similar quality to coal as a referential conventional solid fuel and can be considered as a perspective alternative coal-like combustible fuel source.

To depict the effect of HTT processing temperature on the resultant biochar molar ratio change, the van Krevelen diagram was prepared (Fig. 4). Both molar ratios of O/C and H/C of biochars were significantly lower compared to the feedstock, which suggests the occurrence of a profound deoxygenation reaction *via* both dehydration and decarboxylation routes during the hydrothermal processing of cherry pomace. It can be noticed that the drop in H/C is much more pronounced at higher reaction temperatures, so decarboxylation/decarbonylation as a deoxygenation route appears to be more intensive at lower processing temperatures, while dehydration at higher ones. At the initial stage of conversion, the intensive hydrolysis reactions undergo, what causes the production of water-soluble organics and partial decomposition of the formed by-products. It is also pertinent to mention that the resultant biochars exhibit significantly higher energetic values, so hydrothermal processing caused distinguished energy densification. Particularly, the HHV of biochars obtained at 275 and 350 °C were high (ca. 30 MJ/kg), being comparable to solid fossil fuels.

3.2.2. DRIFT study

DRIFT spectra collected for chosen HTT biochars are depicted in Fig. 5. As seen, the chemical character of the product does not change significantly with the increase in the HTT processing temperature, however, some differences are obvious at a glance. The characteristic broad band at 3000–3700 cm^{-1} is assigned to phenolic –OH vibrations. Higher relative intensity of this band noticed for the samples produced at 350 °C and 275 °C may suggest that their chemical character is more similar to polyphenolic compounds than HTT char obtained at 200 °C. The complex of four overlapping bands at 2800–3000 cm^{-1} is assigned to the symmetric and asymmetric stretching vibrations of aliphatic methyl and methylene groups. This region features higher intensity for the biochar manufactured at 200 °C. Taking into account the lower degree of conversion of the original organic matter in this case, such observation is not surprising. The third region of high absorbance is seen for both samples within 1500–1650 cm^{-1} and corresponds to the vibrations of the aromatic rings in the biochar structures [51,52].

3.2.3. Morphology and textural parameters of biochars

The morphology of the hydrothermal biochars was investigated by means of SEM imaging (Fig. 6). As can be seen in, the solid residue obtained after conversion at 200 °C resulted in a bigger size of, say, flake-shaped particles. This is an indicative which provides that under those conditions only a minor parts of a raw material underwent hydrolysis followed by a deeper decomposition. Indeed, in these conditions only the macromolecules most prone to hydrolysis undergo depolymerization. The particle size does not exceed 100 μm, and the surface of grains of the material is relatively flat. The SEM images taken for the sample prepared at 350 °C (Fig. 6) indicate that the morphology of HTT biochars obtained from cherry pomace is noticeably influenced by the processing temperature. Namely, the increase in hydrothermal treatment temperature entails deep disintegration of the solid raw material. Thus, this biochar reveals a smaller particle sizes of several or several dozen μm. Furthermore, the particles' surface appears to be more rough compared to the biochar obtained at 200 °C. This is not surprising when considering the profound decomposition at higher HTT temperature.

The measurements of low-temperature adsorption of nitrogen (see Fig. 7) revealed that the biochars are low-surface materials with poor porosity. Namely, the BET surface varied between 11 and 13 $m^2\ g^{-1}$ (note, the higher HTT temperature, the lower specific surface area), while V_t reached 0.02–0.04 $cm^3\ g^{-1}$ (similarly, the higher HTT temperature, the lower V_t). The share of microporosity is negligible for all materials (does not exceed 5%). The high-pressure hysteresis loops (p/p_0 = 0.9–1.0) observed for all recorded isotherms suggest the presence of a secondary meso/

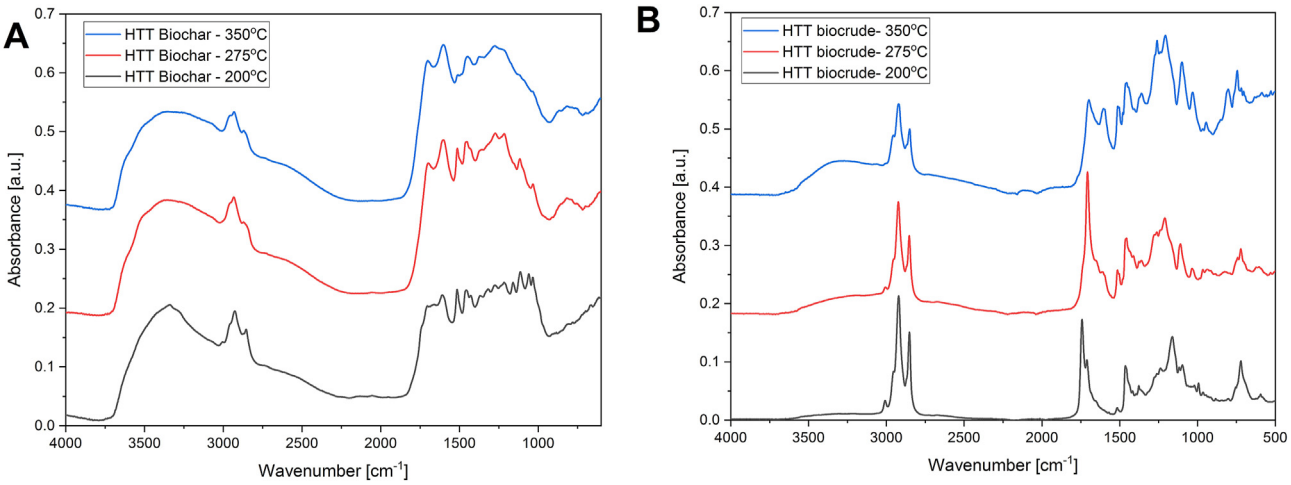

Fig. 5. DRIFT spectra of HTT biochars (A) and ATR-FTIR spectra of biocrudes (B) obtained at different processing temperatures.

macroporosity, which may be formed in the interparticle voids created by the coalescence of the biochar's grains. Indeed, notwithstanding the HTT temperature, the pore size distributions depicted in Fig. 7B clearly show the maxima centered at ca. 24 nm with minor contributions of smaller channels.

3.3. Composition of other HTT group of products

3.3.1. HTT biocrude

The biocrudes obtained through hydrothermal processing were highly viscous and dark in color liquids. The HHV of the resultant liquids varied between 31 and 35 MJ kg^{-1}. The relatively high energy density is the result of a noticeable increase of C content (65–71 wt%) and H content (8–9 wt%) compared to raw material (cf. Table 2). As can be seen on the van Krevelen diagram (cf. Fig. 4), the HHV of biocrudes increased at elevated HTT processing temperatures as a result of gradual deoxygenation. It is also worth noting that O/C is significantly lower compared to the feedstock. It can be also noted that for biocrudes obtained at 350 °C, H/C ratio increased when compared to other samples. Based on the shape of absorption bands of collected spectra for biocrudes obtained at different temperatures, it can be concluded that all samples demonstrate similar qualitative compositions and indicate the presence of aromatic structures, especially phenols, as well as numerous oxygen-containing compounds (carboxylic acids, ketones, aldehydes). However, it can be clearly seen that the increase of HTT temperature resulted in the change of intensity of some characteristic absorption bands, i.e., more pronounced –OH stretching band (3200–3600 cm^{-1}) and carbon-carbon stretches in an aromatic ring (1500, 1460 cm^{-1}) as well as weaker ones of carbonyl group (ca. 1720 cm^{-1}), and C–H stretching vibrations (3000–2800 cm^{-1}). It could be the result of increasing the concentration of phenol derivatives in the biocrude in line with the reduction of carboxylic acids and aldehydes. Those observations are consistent with the GC-MS analysis of the light fractions of the biocrudes (i.e., these with a boiling temperature up to approx. 300 °C) which was presented in Table 3.

3.3.2. HTT gas products

Generally, the dominant component of the gas phase was carbon dioxide. This observation might confirm that decomposition of cherry pomace in subcritical water occurs *via* intensive decarboxylation. In lower concentrations, there were also detected certain amounts of flammable components like methane, propane, n-butane, iso-propane, and n-propane. The increase in processing temperature resulted in a bigger share of combustible components. Particularly, the highest tested temperature (350 °C) caused the more intensive formation of heavier hydrocarbons. It could be caused by undergoing reactions to a greater extent through the radical mechanism than the ionic, what facilitates the production of light molecular mass compounds forming the gas phase. As a result, the non-condensable gas mixture formed at 350 °C features more than 4 times higher heating value than the mixture formed at 200 °C. The composition of the gas phases obtained at various conditions was gathered in Table 4. These findings were similar to research carried out with other types of biomass in subcritical water [53].

3.3.3. Energy recovery

The distribution of energy recovery and C element in the obtained groups of products *via* the hydrothermal treatment of cherry pomace was presented in Fig. 8. The highest energy recovery revealed the biochars, which constituted between 40.4 and 63.0% of the energy accumulated in the raw material. The total energy recovery in the form of HTT group of products varied from 81 to 86% with respect to the pristine feedstock. Taking into account the two-stage approach proposed herein, it is worth noting that the biocrude and gas phase as a source of generation of internal heat within the technology comprises in summary ca. 35, 31, and 15%, in case of processing at 350, 275, and 200 °C, respectively. The high energy recovery proves that hydrothermal treatment may be a promising way for the pretreatment of wet residual matter like cherry pomace before further downstream processing *via* conventional thermochemical routes. The C element balance closure falls within 87.8–98.2 wt% (Fig. 8B). The increase in HTT processing temperature resulted in a gradual diminishing of C share in solid products accompanied by the increment in the form of volatile compounds.

3.4. HTT biochar gasification

As a result of heating up to 1000 °C in carbon dioxide, the biochars underwent a set of reactions of pyrolysis and gasification characteristic for the thermal decomposition of organic materials. The mass losses resulting from these reactions are illustrated in Fig. 9. The pyrolysis step, i.e., thermal decomposition of the samples, started at a temperature of about 300 °C and lasted until ca. 840 °C. The slopes of the TG curves in this temperature range were

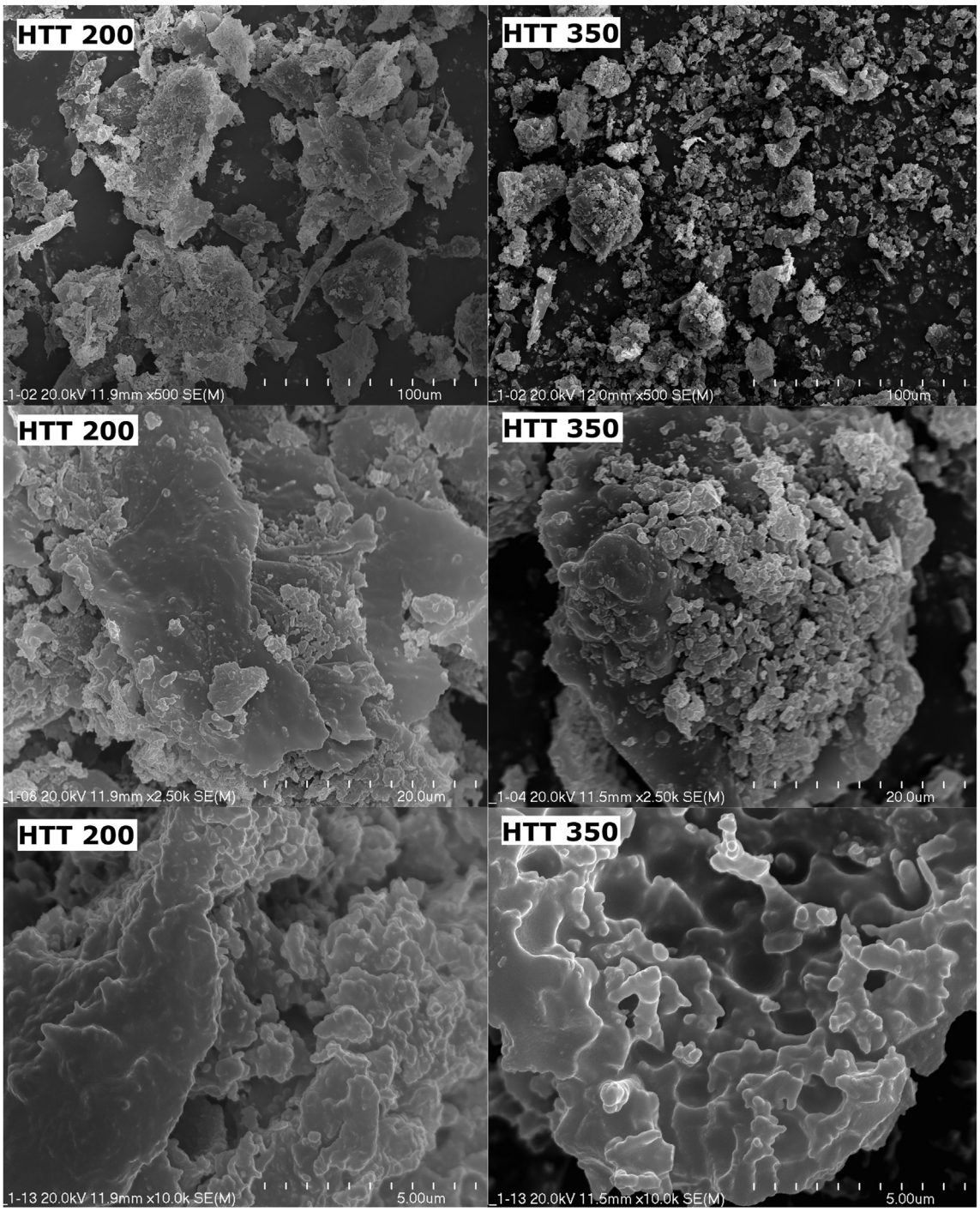

Fig. 6. SEM images of HTT biochars from cherry pomace obtained at 200 °C and 350 °C.

not uniform (at about 500 °C, the inflection of the curve is observed), indicating the differences in the kinetics of the occurring reactions. The devolatilization step can be divided into two ranges, i.e., 300–500 °C and 500–840 °C. At those steps, clear differences between tested biochars can be distinguished. The slopes of the curves of the biochars are different, indicating different reactivity of the materials at this stage. Namely, the highest reactivity is observed for the biochar obtained at 200 °C, whereas the other two samples (i.e., obtained at 275 and 350 °C) demonstrate much lower reactivity. As a consequence, these materials are deeper devolatilized. It is evidenced on DTG curves (cf. Fig. 9 B), where in this region relatively strong peak at 430 °C for the biochar derived at 200 °C can be noticed. For the biochars obtained at higher processing temperatures, the corresponding peaks are much less pronounced and additionally shifted towards higher temperatures, i.e. 479 and 486 °C for samples obtained at 275 and 350 °C, respectively. It can be assigned to the devolatilization of residual, more thermally resistant components, e.g. these ones originating from lignocellulosic structures. This is in line with the ultimate and elemental analysis of biochars, which disclosed a significant decrease in the volatile matter, increase in fixed carbon and elemental carbon along with rising HTT temperature. Moreover, it is also worth

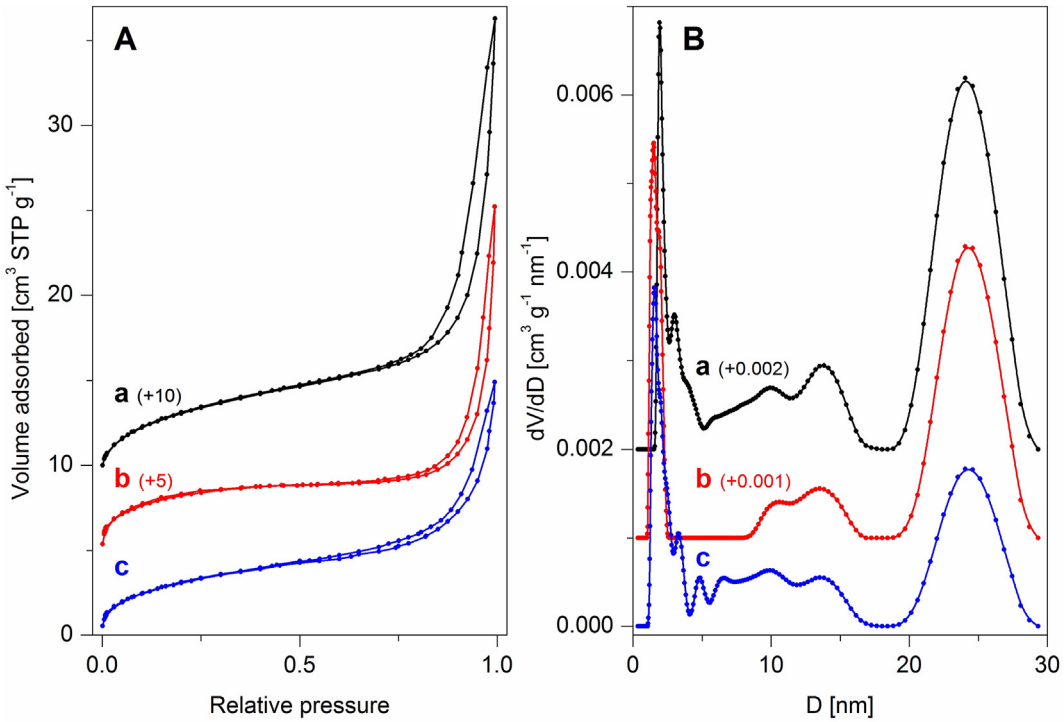

Fig. 7. Low-temperature isotherms (A), and corresponding pore size distributions (B) for the biochars obtained by HTT of cherry pomace at 200 °C (a), 275 °C (b), and 350 °C (c).

pointing out that carbonaceous materials that are generated at more severe HTT conditions reveal higher thermal stability of the biochar's structure. This in turn can be clearly seen by the further tailing of the peak until the beginning of the gasification stage at around 840 °C. The increasing aromaticity of solid products obtained under harsher conditions was proven by DRIFT analysis as well as a gradual decrease in H/C and O/C ratios.

The residual part of the biochars changing from 32 wt% for HTT200 biochar to 54 wt% for HTT350 biochar undergoes a gasification reaction with carbon dioxide which starts at about 840 °C. At this step, differences in curve's slopes are also observed, which indicates differences in reactivity of the chars. The information presented above is summarized in Table 5.

The differences observed can be explained by the different "thermal histories" of the biochars. Namely, the most reactive at the devolatilization step and resulting in the smallest mass of char at the gasification step is the biochar from the HTT process conducted at the lowest temperature i.e. 200 °C. Contrarily, the least reactive at the pyrolysis step, resulting in the highest mass of char at the gasification step is the biochar produced by the HTT process performed at the highest temperature i.e. 350 °C. Generally, it can be stated that the temperature of HTT process determines the reactivity of the biochar for further thermochemical processing, wherein the higher temperature of HTT process, the lower reactivity of the resulting biochar. Moreover, the increase in HTT process temperature causes a reduction in the pyrolysis mass loss in favor of the gasification. It is known that the gasification rate depends strongly on the internal diffusion limitation inside the material particles. As was evidenced in Section 3.2, the resultant biochars are low-surface materials with poorly developed porosity. Additionally, it was found that biochars obtained at higher temperatures exhibit slightly lower specific surface areas. It is also pertinent to mention that the devolatilization stage can affect also the properties of the resultant biochar which is next subjected to gasification. Taking into account that during the pyrolysis stage, the highest pronounced changes occur for the biochar obtained at the lowest temperature (200 °C), one may infer that some structural changes may occur (e.g. creation of some new pores or enlargement of the existing ones), which in consequence develop the porosity in the bigger matter than for biochars obtained at higher HTT temperatures. This in turn can affect the acceleration of gasification and may result in lowering its activation energy. Furthermore, according to Ulbrich et al. [54], gasification reactivity depends not only on porous structure but it is also influenced by the nature of the carbonaceous structures, i.e., carbon sites, edges, dislocations, and other structure defects. Thus, it is plausible that gasification reactivity could be more dependent on the lesser availability of the active sites with the increase of the proven aromaticity for samples obtained at higher HTT temperatures, which was also formerly postulated by Zhuang et al. [55].

In the next step, the kinetic parameters of the gasification process were calculated to quantitatively describe the process. The selection of the Coats-Redfern method is justified by the fact that this approach, just after the Senum & Young method, provides the lowest uncertainty resulting from the approximation of the p(x) integral solution for a wide range of $x = E/(RT)$ values and is much easier to implement than Senum & Young approach. The values of kinetic parameters and reaction order are summarized in Table 6, whereas the fitting of the model to the experimental data is illustrated in Fig. 10. The values of the reaction order providing the best fit of the model to the experimental data are equal 1.8 for all biochars tested. This value is close to 2, which is considered as one of the values having a chemical basis [41]. Both values, activation energies and the pre-exponential factors, are relatively high when compared with the values typically reported for coal [56] and biomass [57–59]. It could be connected with low ash content in case of transformed cherry pomace and as a consequence a negligible catalytic effect. Additionally, during HTT some mineral matter is transferred to the aqueous phase (by leaching), what could additionally diminish the potential effect. This curious effect

Table 3
Compounds identified in HTT biocrude obtained at different processing temperatures.

RT (min)	Compound	200 °C	275 °C	350 °C
14.776	2-Pentanone, 4-hydroxy-4-methyl-	0.54%	0.56%	0.51%
16.929	3-Furaldehyde	11.97%	–	–
17.620	2-Cyclopenten-1-one	–	–	0.19%
19.449	2-Propanone, 1-(acetyloxy)-	0.24%	–	–
20.105	Pyridine, 2,5-dimethyl-	–	–	0.13%
20.716	2-Cyclopenten-1-one, 2-methyl-	–	0.55%	0.63%
21.087	Ethanone, 1-(2-furanyl)-	0.23%	–	0.17%
23.096	2,5-Hexanedione	0.13%	–	–
23.899	Benzaldehyde	0.34%	–	–
24.100	Phenol	0.22%	0.84%	2.17%
24.454	2-Furancarboxaldehyde, 5-methyl-	3.12%	–	–
24.970	2-Cyclopenten-1-one, 3-methyl-	–	–	0.97%
25.035	Butanoic acid, 4-hydroxy-	0.15%	–	0.51%
24.943	2-Cyclopenten-1-one, 3,4-dimethyl-	–	0.37%	0.22%
25.420	2-Cyclopenten-1-one, 2,3-dimethyl-	–	0.21%	0.23%
26.459	Pyridine, 3-methoxy-	–	–	0.66%
27.463	2-Cyclopenten-1-one, 2-hydroxy-3-methyl-	1.07%	0.50%	0.20%
27.778	2-Hexenal, 2-ethyl-	–	0.24%	–
27.869	1H-Pyrrole-2-carboxaldehyde	1.94%	–	–
28.035	Benzyl alcohol	0.42%	–	–
28.053	1-Methoxy-1,4-cyclohexadiene	–	0.97%	2.40%
28.651	Furaneol	0.23%	–	–
28.970	Propanoic acid, 2-(phenylmethoxy)-	0.17%	–	–
29.014	p-Cresol	–	0.30%	1.19%
29.215	2-Furancarboxylic acid	1.03%	–	–
30.411	Bicyclo[2.2.1]heptane, 2,2,3-trimethyl-	0.58%	–	–
30.678	Phenol, 2-methoxy-	1.39%	5.70%	9.01%
31.717	2-Cyclopenten-1-one, 3-ethyl-2-hydroxy-	0.19%	0.30%	0.16%
32.141	3-Pyridinol	2.23%	–	2.65%
32.481	2-Propenal, 3-(2-furanyl)-	0.12%	–	–
32.957	2,5-Furandicarboxaldehyde	0.40%	–	–
33.158	2(1H)-Pyridone, 6-methyl-	–	–	0.29%
33.634	Phenol, 3-ethyl-	–	0.30%	0.30%
35.228	2-Methoxy-5-methylphenol	–	0.68%	3.00%
36.346	Catechol	1.88%	2.13%	4.84%
38.574	Benzeneacetic acid	0.14%	0.22%	–
38.762	Propanedioic acid, phenyl-	–	–	0.22%
38.936	Phenol, 4-ethyl-2-methoxy-	0.14%	1.70%	2.03%
39.897	Resorcinol, 2-acetyl-	0.58%	0.37%	0.30%
40.033	1,2-Benzenediol, 3-methoxy-	0.32%	0.56%	7.78%
40.561	5-Hydroxymethylfurfural	8.56%	–	–
41.731	Hydroquinone	–	–	0.61%
42.111	Benzenepropanoic acid, octyl ester	–	0.21%	0.38%
42.426	Phenol, 2-methoxy-4-propyl-	0.47%	0.59%	0.71%
43.740	Benzenemethanol,.alpha.-ethyl-4-methoxy-	0.12%	0.21%	0.36%
44.666	1,3-Benzenediol, 2-methyl-	–	–	0.79%
45.042	Phenol, 2,6-dimethoxy-	2.30%	9.64%	11.22%
46.989	3-Allyl-6-methoxyphenol	0.79%	0.65%	0.52%
47.474	Vanillin	3.17%	0.87%	1.22%
48.343	2,3-Dimethoxybenzyl alcohol	0.13%	1.14%	2.16%
49.876	Corymbolone	0.17%	–	–
51.112	5-tert-Butylpyrogallol	–	1.66%	1.63%
51.715	1,4-Benzenediol, 2,3,5-trimethyl-	–	–	0.27%
52.724	2-Propanone, 1-(4-hydroxy-3-methoxyphenyl)-	1.78%	1.71%	1.03%
53.846	2,4-Hexadienedioic acid, 3,4-diethyl-, dimethyl ester, (Z,Z)-	–	0.91%	0.96%
54.790	Pyridine, 2-(1-propylbutyl)-	–	0.26%	0.14%
56.838	Benzenepropanol, 4-hydroxy-3-methoxy-	2.87%	1.19%	1.87%
57.222	Phenol, 2,6-dimethoxy-4-(2-propenyl)-	–	0.27%	0.39%
57.589	2-Allyl-3,6-dimethoxybenzyl alcohol	–	–	0.25%
58.074	Pentadecanoic acid, 13-methyl-, methyl ester	1.14%	1.40%	0.28%
58.786	3,5-Dimethoxy-4-(isopropyl)oxybenzaldehyde	4.15%	0.37%	0.34%
59.987	Phorbol	2.08%	5.91%	1.98%
62.607	Desaspidinol	1.78%	1.54%	0.37%
66.180	Oleic Acid	3.57%	20.26%	6.42%
66.708	Linoleic acid	3.22%	16.81%	2.71%

inspired us to deepen the study on the chemical nature of the mineral part in the resultant biochars. The ash samples from raw material and obtained biochars were analyzed by XRF and FT-IR (DRIFT) spectroscopy (cf. Appendix A, Table A.1. and Fig. A.2.). It was found that mineral parts of HTT biochars are likely to be significantly depleted of alkaline elements. This is caused by etching them from the processed biomass into the HTT medium, especially in the form of soluble bicarbonates of alkaline elements (e.g., potassium and magnesium). As consequence after process, the ash is enriched in various phosphates/hydroxyphosphates species. Ultimately, since the alkali metals are believed to play the catalytic role in the gasification of biochars, the absence of them in the

Table 4
Composition of HTT gaseous phase obtained at different temperatures.

Compound	Concentration [wt%]		
	200 °C	275 °C	350 °C
CO_2	91.18	82.15	61.47
CH_4	3.70	13.14	10.89
C_2	–	0.44	5.02
C_3	1.70	1.51	7.98
C_4	1.55	2.25	11.27
C_5	1.87	0.53	3.38
HHV [MJ m^{-3}]	8.43	10.91	36.20

biochars affects the activation energy of gasification causing it to be higher. The detailed discussion and results in this matter were presented in Appendix A. To reduce the E_a, the effect of co-processing with higher ash content material, e.g., microalgae, could be investigated.

It is worth emphasizing that the use of the n-th reaction order was to better match the model data with the experimental ones, not to determine the reaction order *sensu stricto*. The parameter n should be considered here as a constant of the equation, rather than the exact reaction order. It can be stated that the compensation effect [60] is observed, which means that the high values of activation energies are compensated by very high values of pre-exponential factors.

The match factor between the model data calculated based on kinetic parameters and the experimental data is satisfactory. The largest deviations (however, not exceeding 10%) are observed for low conversion rates (Fig. 10).

4. Conclusion

Nowadays, the wet residual matter generated by the food industry like fruit and vegetable pomaces do not find efficient disposal routes. The direct utilization of this kind of residues through conventional technologies like pyrolysis and gasification could be problematic and expensive. Thus, we proposed a two-stage processing route consisting of hydrothermal treatment followed by gasification for the conversion of high-moisture-containing organic matter towards synthetic gas. At the first stage, we have investigated the effect of hydrothermal treatment processing temperature on the yield and quality of biochar as the target bioproduct. The biochars produced from cherry pomace

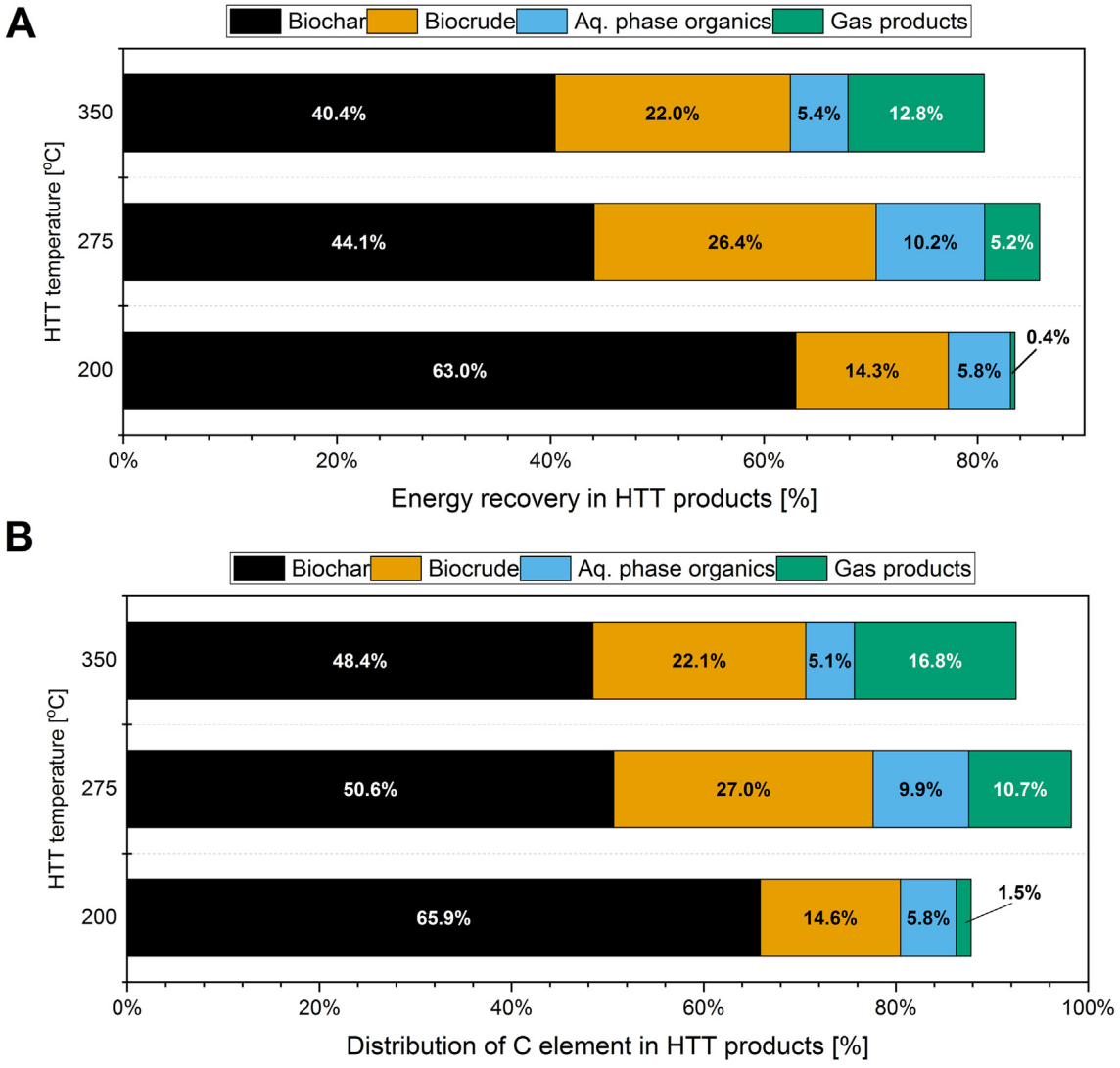

Fig. 8. Energy recovery (A) and distribution of C element (B) in HTT group of products.

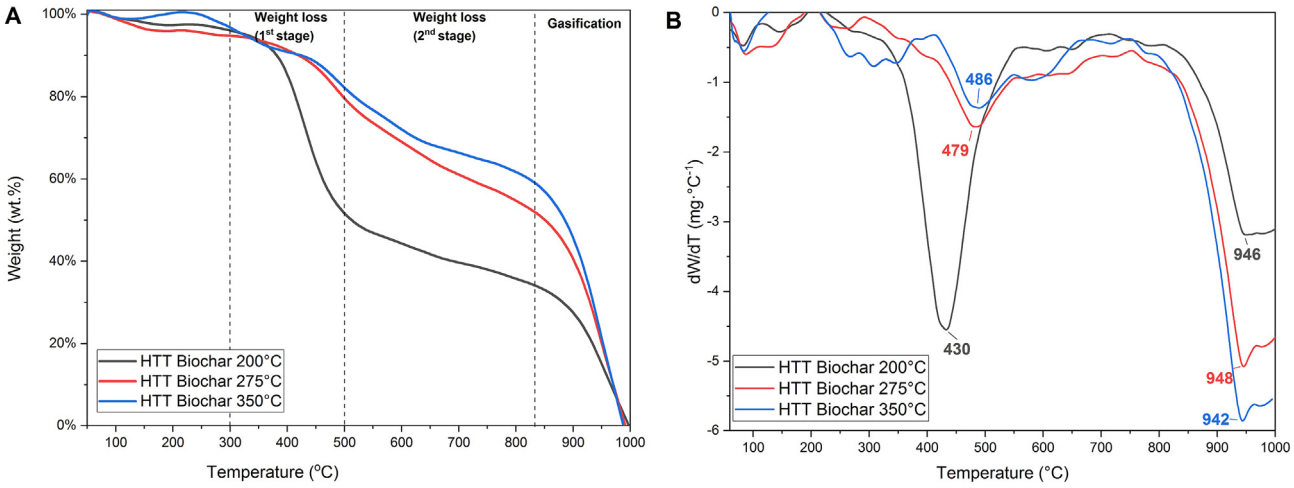

Fig. 9. TG (A) and DTG (B) curves of the tested biochars recorded under CO_2 atmosphere.

Table 5
Comparison of the TG measurement stages.

Step		HTT biochar		
		200 °C	275 °C	350 °C
Weight loss (1st stage)	t_b, °C	300	300	300
	t_f, °C	500	500	500
	Δm, wt%	52	28	25
Weight loss (2nd stage)	t_b, °C	500	500	500
	t_f, °C	840	840	840
	Δm, wt%	13	27	18
Gasification	t_b, °C	840	840	840
	t_f, °C	990	990	990
	Δm, wt%	32	42	54

t_b – starting temperature, t_f – final temperature, Δm – mass loss.

Table 6
Kinetic parameters calculated from nth order (Coats-Redfern approximation).

Parameter		HTT biochar		
		200 °C	275 °C	350 °C
Reaction order (n)	–	1.8	1.8	1.8
Activation energy (E_a)	kJ mol^{-1}	732	668	691
Pre-exponential factor (A)	s^{-1}	$3.25 \cdot 10^{31}$	$4.19 \cdot 10^{28}$	$4.51 \cdot 10^{29}$

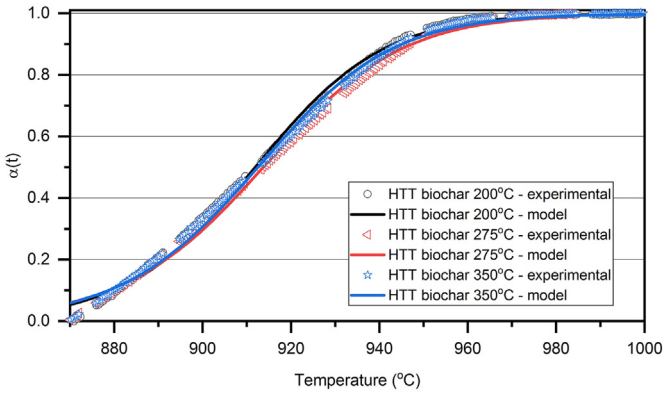

Fig. 10. Fitting of the kinetic model to the experimental data.

exhibit a noticeable increase in carbon content compared to raw material. Moreover, the quality of biochars appears to be comparable to those obtained from dedicated energy crops. Raising the processing temperature to 350 °C resulted in changes in the structure of the resultant solid product as was proven by means of DRIFT and TG analysis. Subsequently, we have investigated the kinetics of gasification under CO_2 of biochars obtained at various conditions. We have found that the reactivity of the biochar depends on the hydrothermal treatment temperature. The higher the temperature of HTT process, the lower reactivity of the resulting biochar. The presented research allowed us to consider the proposed two-stage concept as a promising approach for wet organic matter utilization. It seems that low-temperature hydrothermal treatment followed by biochar gasification under CO_2 could be a prospective route for the conversion of wet residuals generated, e.g., by the food industry. However, deeper investigation in this

field is necessary. For instance, it would be expedient to investigate the quality and quantity of syngas produced from HTT biochar. Additionally, it was evidenced that HTT biochar from cherry pomace may be a valuable intermediate, which could be further upgraded to value-added final products.

CRediT authorship contribution statement

Mariusz Wądrzyk: Conceptualization, Investigation, Formal analysis, Visualization, Writing – original draft, preparation, Funding acquisition. **Przemysław Grzywacz:** Investigation, Writing – review & editing. **Rafał Janus:** Investigation, Writing – review & editing. **Marek Michalik:** Investigation.

Declaration of competing interest

The authors declare that they have no known competing financial interests or personal relationships that could have appeared to influence the work reported in this paper.

Acknowledgement

This paper was prepared as a part of the research subsidy of the Faculty of Energy and Fuels at the AGH University of Science and Technology under project number 16.16.210.476. The research was carried out using the infrastructure of the AGH Centre of Energy, AGH University of Science and Technology. The authors gratefully acknowledge Tymbark - MWS company (Tymbark, Poland) for supplying the feedstock and fruitful cooperation.

Appendix A. Supplementary data

Supplementary data to this article can be found online at https://doi.org/10.1016/j.renene.2021.06.130.

References

[1] Eurostat, The Fruit and Vegetable Sector in the EU - a Statistical Overview, 2019.
[2] U.S.D. of A. Carmen Valverde, Stone fruit annual - European union, report number e42020-0052. https://apps.fas.usda.gov/newgainapi/api/Report/DownloadReportByFileName?fileName=Stone%20Fruit%20Annual_Madrid_European%20Union_08-26-2020, 2020.
[3] U. Balon, J.M. Dziadkowiec, Polski rynek soków, naktarów i napojów, in: Jakość z punktu widzenia konsum. i organ. rynek soków, nektarów i napojów, Red. Sikora T., Wyd. Nauk. Akapit, 2016, pp. 49–69.
[4] G.S. Dhillon, S. Kaur, S.K. Brar, Perspective of apple processing wastes as low-cost substrates for bioproduction of high value products: a review, Renew. Sustain. Energy Rev. 27 (2013) 789–805, https://doi.org/10.1016/j.rser.2013.06.046.
[5] G.S. Dhillon, S.K. Brar, M. Verma, R.D. Tyagi, Enhanced solid-state citric acid bio-production using apple pomace waste through surface response methodology, J. Appl. Microbiol. 110 (2011) 1045–1055, https://doi.org/10.1111/j.1365-2672.2011.04962.x.
[6] B. Gullón, R. Yanez, J.L. Alonso, J.C. Parajó, L -Lactic acid production from apple pomace by sequential hydrolysis and fermentation, Bioresour. Technol. 99 (2008) 308–319, https://doi.org/10.1016/j.biortech.2006.12.018.
[7] G. Ćetković, J. Canadanović-Brunet, S. Djilas, S. Savatović, A. Mandić, V. Tumbas, Assessment of polyphenolic content and in vitro antiradical characteristics of apple pomace, Food Chem. 109 (2008) 340–347, https://doi.org/10.1016/j.foodchem.2007.12.046.
[8] Y. Lu, L.Y. Foo, Identification and quantification of major polyphenols in apple pomace, Food Chem. 59 (1997) 187–194, https://doi.org/10.1016/S0308-8146(96)00287-7.
[9] N. Gao, X. Sun, D. Li, E. Gong, J. Tian, X. Si, X. Jiao, J. Xing, Y. Wang, X. Meng, B. Li, Optimization of anthocyanidins conversion using chokeberry pomace rich in polymeric proanthocyanidins and cellular antioxidant activity analysis, LWT 133 (2020), https://doi.org/10.1016/j.lwt.2020.109889, 109889.
[10] C. Beres, G.N.S. Costa, I. Cabezudo, N.K. da Silva-James, A.S.C. Teles, A.P.G. Cruz, C. Mellinger-Silva, R.V. Tonon, L.M.C. Cabral, S.P. Freitas, Towards integral utilization of grape pomace from winemaking process: a review, Waste Manag. 68 (2017) 581–594, https://doi.org/10.1016/j.wasman.2017.07.017.
[11] F. Masoodi, B. Sharma, G.S. Chauhan, Use of apple pomace as a source of dietary fiber in cakes, Plant Foods Hum. Nutr. 57 (2002) 121–128, https://doi.org/10.1023/A:1015264032164.
[12] H. Chen, G.L. Rubenthaler, E.G. Schanus, Effect of apple fiber and cellulose on the physical properties of wheat flour, J. Food Sci. 53 (1988) 304–305, https://doi.org/10.1111/j.1365-2621.1988.tb10242.x.
[13] F. Streit, F. Koch, M.C.M. Laranjeira, J.L. Ninow, Production of fungal chitosan in liquid cultivation using apple pomace as substrate, Braz. J. Microbiol. 40 (2009) 20–25, https://doi.org/10.1590/S1517-83822009000100003.
[14] M. Stredansky, E. Conti, Xanthan production by solid state fermentation, Process Biochem. 34 (1999) 581–587, https://doi.org/10.1016/S0032-9592(98)00131-9.
[15] M.O. Ngadi, L.R. Correia, Kinetics of solid-state ethanol fermentation from apple pomace, J. Food Eng. 17 (1992) 97–116, https://doi.org/10.1016/0260-8774(92)90055-B.
[16] J.A.S. Mendes, A.M.R.B. Xavier, D.V. Evtuguin, L.P.C. Lopes, Integrated utilization of grape skins from white grape pomaces, Ind. Crop. Prod. 49 (2013) 286–291, https://doi.org/10.1016/j.indcrop.2013.05.003.
[17] L.J.R. Nunes, L.M.E.F. Loureiro, L.C.R. Sá, H.F.C. Silva, Evaluation of the potential for energy recovery from olive oil industry waste: thermochemical conversion technologies as fuel improvement methods, Fuel 279 (2020) 118536, https://doi.org/10.1016/j.fuel.2020.118536.
[18] EU, Directive (EU) 2018/2001 of the European Parliament and of the Council on the promotion of the use of energy from renewable sources, Off. J. Eur. Union 2018 (2018) 82–209.
[19] S.N. Naik, V.V. Goud, P.K. Rout, A.K. Dalai, Production of first and second generation biofuels: a comprehensive review, Renew. Sustain. Energy Rev. 14 (2010) 578–597, https://doi.org/10.1016/j.rser.2009.10.003.
[20] A. Meng, S. Chen, Y. Long, H. Zhou, Y. Zhang, Q. Li, Pyrolysis and gasification of typical components in wastes with macro-TGA, Waste Manag. 46 (2015) 247–256, https://doi.org/10.1016/j.wasman.2015.08.025.
[21] A.V. Bridgwater, Review of fast pyrolysis of biomass and product upgrading, Biomass Bioenergy 38 (2012) 68–94, https://doi.org/10.1016/j.biombioe.2011.01.048.
[22] M. Wądrzyk, R. Janus, B. Rządzik, M. Lewandowski, S. Budzyń, Pyrolysis oil from scrap tires as a source of fuel components: manufacturing, fractionation, and characterization, Energy Fuels 34 (2020) 5917–5928, https://doi.org/10.1021/acs.energyfuels.0c00265.
[23] A.V. Bridgwater, Principles and practice of biomass fast pyrolysis processes for liquids, J. Anal. Appl. Pyrolysis 51 (1999) 3–22, https://doi.org/10.1016/S0165-2370(99)00005-4.
[24] V. Dhyani, T. Bhaskar, A comprehensive review on the pyrolysis of lignocellulosic biomass, Renew. Energy 129 (2018) 695–716, https://doi.org/10.1016/j.renene.2017.04.035.
[25] X. Zhang, H. Deng, X. Hou, R. Qiu, Z. Chen, Pyrolytic behavior and kinetic of wood sawdust at isothermal and non-isothermal conditions, Renew. Energy 142 (2019) 284–294, https://doi.org/10.1016/j.renene.2019.04.115.
[26] C. Quan, Z. Ma, N. Gao, C. He, Pyrolysis and combustion characteristics of corncob hydrolysis residue, J. Anal. Appl. Pyrolysis 130 (2018) 72–78, https://doi.org/10.1016/j.jaap.2018.01.025.
[27] C. Quan, A. Bieniek, A. Magdziarz, N. Gao, M. Śliz, Biomass CO_2 gasification with CaO looping for syngas production in a fixed-bed reactor, Renew. Energy 167 (2021) 652–661, https://doi.org/10.1016/j.renene.2020.11.134.
[28] M.A. Hamad, A.M. Radwan, D.A. Heggo, T. Moustafa, Hydrogen rich gas production from catalytic gasification of biomass, Renew. Energy 85 (2016) 1290–1300, https://doi.org/10.1016/j.renene.2015.07.082.
[29] A.A. Peterson, F. Vogel, R.P. Lachance, M. Fröling, M.J. Antal, J.W. Tester, Thermochemical biofuel production in hydrothermal media: a review of sub- and supercritical water technologies, Energy Environ. Sci. 1 (2008) 32–65, https://doi.org/10.1039/b810100k.
[30] A.R.K. Gollakota, N. Kishore, S. Gu, A review on hydrothermal liquefaction of biomass, Renew. Sustain. Energy Rev. 81 (2018) 1378–1392, https://doi.org/10.1016/j.rser.2017.05.178.
[31] M. Wądrzyk, R. Janus, J. Jakóbiec, Liquefaction of waste organic matter towards bio-oil in subcritical water, Przem. Chem. 96 (2017), https://doi.org/10.15199/62.2017.9.19.
[32] K. Tekin, S. Karagöz, S. Bektaş, A review of hydrothermal biomass processing, Renew. Sustain. Energy Rev. 40 (2014) 673–687, https://doi.org/10.1016/j.rser.2014.07.216.
[33] J. Akhtar, N. Saidina Amin, A review on operating parameters for optimum liquid oil yield in biomass pyrolysis, Renew. Sustain. Energy Rev. 16 (2012) 5101–5109, https://doi.org/10.1016/j.rser.2012.05.033.
[34] S.S. Toor, L. Rosendahl, A. Rudolf, Hydrothermal liquefaction of biomass: a review of subcritical water technologies, Energy 36 (2011) 2328–2342, https://doi.org/10.1016/j.energy.2011.03.013.
[35] M. Gong, W. Zhu, Z.R. Xu, H.W. Zhang, H.P. Yang, Influence of sludge properties on the direct gasification of dewatered sewage sludge in supercritical water, Renew. Energy 66 (2014) 605–611, https://doi.org/10.1016/j.renene.2014.01.006.
[36] M.P. Olszewski, P.J. Arauzo, M. Wądrzyk, A. Kruse, Py-GC-MS of hydrochars produced from brewer's spent grains, J. Anal. Appl. Pyrolysis 140 (2019) 255–263, https://doi.org/10.1016/j.jaap.2019.04.002.
[37] M.P. Olszewski, P.J. Arauzo, P.A. Maziarka, F. Ronsse, A. Kruse, Pyrolysis kinetics of hydrochars produced from brewer's spent grains 9, 625, Catalysts, 2019, pp. 1–22, https://doi.org/10.3390/catal9070625.
[38] X. Zhuang, Y. Song, H. Zhan, X. Yin, C. Wu, Gasification performance of

biowaste-derived hydrochar: the properties of products and the conversion processes, Fuel 260 (2020) 116320, https://doi.org/10.1016/j.fuel.2019.116320.
[39] C. Lin, J. Zhang, P. Zhao, Z. Wang, M. Yang, X. Cui, H. Tian, Q. Guo, Gasification of real MSW-derived hydrochar under various atmosphere and temperature, Thermochim. Acta 683 (2020) 178470, https://doi.org/10.1016/j.tca.2019.178470.
[40] M. Wądrzyk, R. Janus, M.P. Vos, D.W.F. Brilman, Effect of process conditions on bio-oil obtained through continuous hydrothermal liquefaction of *Scenedesmus* sp . microalgae, J. Anal. Appl. Pyrolysis 134 (2018) 415–426, https://doi.org/10.1016/j.jaap.2018.07.008.
[41] J.E. House, Principles of Chemical Kinetics, second ed., 2007.
[42] S.R. Naqvi, R. Tariq, Z. Hameed, I. Ali, M. Naqvi, W.-H. Chen, S. Ceylan, H. Rashid, J. Ahmad, S.A. Taqvi, M. Shahbaz, Pyrolysis of high ash sewage sludge: kinetics and thermodynamic analysis using Coats-Redfern method, Renew. Energy 131 (2019) 854–860, https://doi.org/10.1016/j.renene.2018.07.094.
[43] M. Déniel, G. Haarlemmer, A. Roubaud, E. Weiss-Hortala, J. Fages, Optimisation of bio-oil production by hydrothermal liquefaction of agro-industrial residues: blackcurrant pomace (*Ribes nigrum* L .) as an example, Biomass Bioenergy 95 (2016) 273–285, https://doi.org/10.1016/j.biombioe.2016.10.012.
[44] A. Missaoui, S. Bostyn, V. Belandria, B. Cagnon, B. Sarh, I. Gökalp, Hydrothermal carbonization of dried olive pomace: energy potential and process performances, J. Anal. Appl. Pyrolysis 128 (2017) 281–290, https://doi.org/10.1016/j.jaap.2017.09.022.
[45] M. Pala, I.C. Kantarli, H.B. Buyukisik, J. Yanik, Hydrothermal carbonization and torrefaction of grape pomace: a comparative evaluation, Bioresour. Technol. 161 (2014) 255–262, https://doi.org/10.1016/j.biortech.2014.03.052.
[46] D.W.F. Brilman, N. Drabik, M. Wądrzyk, Hydrothermal co-liquefaction of microalgae, wood, and sugar beet pulp, Biomass Convers. Biorefinery. 7 (2017) 445–454, https://doi.org/10.1007/s13399-017-0241-2.
[47] A. Dimitriadis, S. Bezergianni, Hydrothermal liquefaction of various biomass and waste feedstocks for biocrude production: A state of the art review, Renew. Sustain. Energy Rev. 68 (2017) 113–125, https://doi.org/10.1016/j.rser.2016.09.120.
[48] M. Wadrzyk, M. Berdel, R. Janus, D.W.F. Brilman, Hydrothermal processing of pine wood: effect of process variables on bio-oil quality and yield, E3S Web Conf. 108 (2019) 1–11, https://doi.org/10.1051/e3sconf/201910802004.
[49] A. Magdziarz, M. Wilk, M. Wądrzyk, Pyrolysis of hydrochar derived from biomass – experimental investigation, Fuel 267 (2020), https://doi.org/10.1016/j.fuel.2020.117246.
[50] S.V. Vassilev, D. Baxter, L.K. Andersen, C.G. Vassileva, An overview of the chemical composition of biomass, Fuel 89 (2010) 913–933, https://doi.org/10.1016/j.fuel.2009.10.022.
[51] R.R.R. Kannan, R. Arumugam, P. Anantharaman, Fourier transform infrared spectroscopy analysis of seagrass polyphenols, Curr. Bioact. Compd. 7 (2011) 118–125, https://doi.org/10.2174/157340711796011142.
[52] İ. Okur, C. Baltacıoğlu, E. Ağçam, H. Baltacıoğlu, H. Alpas, Evaluation of the effect of different extraction techniques on sour cherry pomace phenolic content and antioxidant activity and determination of phenolic compounds by FTIR and HPLC, Waste Biomass Valoriz. 10 (2019) 3545–3555, https://doi.org/10.1007/s12649-019-00771-1.
[53] L. Garcia Alba, C. Torri, C. Samorì, J. Van Der Spek, D. Fabbri, S.R.A. Kersten, D.W.F. Brilman, Hydrothermal treatment (HTT) of microalgae: evaluation of the process as conversion method in an algae biorefinery concept, Energy Fuels 26 (2012) 642–657, https://doi.org/10.1021/ef201415s.
[54] M. Ulbrich, D. Preßl, S. Fendt, M. Gaderer, H. Spliethoff, Impact of HTC reaction conditions on the hydrochar properties and CO_2 gasification properties of spent grains, Fuel Process. Technol. 167 (2017) 663–669, https://doi.org/10.1016/j.fuproc.2017.08.010.
[55] X. Zhuang, H. Zhan, Y. Song, X. Yin, C. Wu, Structure-reactivity relationships of biowaste-derived hydrochar on subsequent pyrolysis and gasification performance, Energy Convers. Manag. 199 (2019) 112014, https://doi.org/10.1016/j.enconman.2019.112014.
[56] G. Czerski, K. Zubek, P. Grzywacz, S. Porada, Effect of char preparation conditions on gasification in a carbon dioxide atmosphere, Energy Fuels 31 (2017) 815–823, https://doi.org/10.1021/acs.energyfuels.6b02139.
[57] Q. He, Q. Guo, L. Ding, J. Wei, G. Yu, CO_2 gasification of char from raw and torrefied biomass: reactivity, kinetics and mechanism analysis, Bioresour. Technol. 293 (2019), https://doi.org/10.1016/j.biortech.2019.122087.
[58] S. Sobek, S. Werle, Isoconversional determination of the apparent reaction models governing pyrolysis of wood, straw and sewage sludge, with an approach to rate modelling, Renew. Energy 161 (2020) 972–987, https://doi.org/10.1016/j.renene.2020.07.112.
[59] S. Sobek, S. Werle, Kinetic modelling of waste wood devolatilization during pyrolysis based on thermogravimetric data and solar pyrolysis reactor performance, Fuel 261 (2020) 116459, https://doi.org/10.1016/j.fuel.2019.116459.
[60] M.A. Akhtar, S. Zhang, X. Shao, H. Dang, Y. Liu, T. Li, L. Zhang, C.Z. Li, Kinetic compensation effects in the chemical reaction-controlled regime and mass transfer-controlled regime during the gasification of biochar in O_2, Fuel Process. Technol. 181 (2018) 25–32, https://doi.org/10.1016/j.fuproc.2018.09.009.